LYMPHATIC RESEARCH AND BIOLOGY
Volume 15, Number 1, 2017

DOI: 10.1089/lrb.2016.0020

Bilateral Changes in Deep Tissue Environment After Manual Lymphatic Drainage in Patients with Breast Cancer Treatment-Related Lymphedema

Paula M.C. Donahue, PT, DPT, CLT-LANA,[1,2] Rachelle Crescenzi, PhD,[3] Allison O. Scott, BA,[3] Vaughn Braxton, MD,[3] Aditi Desai, MD,[3] Seth A. Smith, PhD,[3] John Jordi, PTA, CT-LANA,[4] Ingrid M. Meszoely, MD,[5] Ana M. Grau, MD,[5] Rondi M. Kauffmann, MD,[5] Raeshell S. Sweeting, MD,[5] Kandace Spotanski, BS,[6] Sheila H. Ridner, PhD, RN, FAAN,[6] and Manus J. Donahue, PhD[3,7–9]

Abstract

Background: Breast cancer treatment-related lymphedema (BCRL) arises from a mechanical insufficiency following cancer therapies. Early BCRL detection and personalized intervention require an improved understanding of the physiological processes that initiate lymphatic impairment. Here, internal magnetic resonance imaging (MRI) measures of the tissue microenvironment were paired with clinical measures of tissue structure to test fundamental hypotheses regarding structural tissue and muscle changes after the commonly used therapeutic intervention of manual lymphatic drainage (MLD).

Methods and Results: Measurements to identify lymphatic dysfunction in healthy volunteers ($n=29$) and patients with BCRL ($n=16$) consisted of (1) limb volume, tissue dielectric constant, and bioelectrical impedance (i.e., non-MRI measures); (2) qualitative 3 Tesla diffusion-weighted, T_1-weighted and T_2-weighted MRI; and (3) quantitative multi-echo T_2 MRI of the axilla. Measurements were repeated in patients immediately following MLD. Normative control and BCRL T_2 values were quantified and a signed Wilcoxon Rank-Sum test was applied (significance: two-sided $p<0.05$). Non-MRI measures yielded significant capacity for discriminating between arms with versus without clinical signs of BCRL, yet yielded no change in response to MLD. Alternatively, a significant increase in deep tissue T_2 on the involved (pre $T_2=0.0371\pm0.003$ seconds; post $T_2=0.0389\pm0.003$; $p=0.029$) and contralateral (pre $T_2=0.0365\pm0.002$; post $T_2=0.0395\pm0.002$; $p<0.01$) arms was observed. Trends for larger T_2 increases on the involved side after MLD in patients with stage 2 BCRL relative to earlier stages 0 and 1 BCRL were observed, consistent with tissue composition changes in later stages of BCRL manifesting as breakdown of fibrotic tissue after MLD in the involved arm. Contrast consistent with relocation of fluid to the contralateral quadrant was observed in all stages.

Conclusion: Quantitative deep tissue T_2 MRI values yielded significant changes following MLD treatment, whereas non-MRI measurements did not vary. These findings highlight that internal imaging measures of tissue composition may be useful for evaluating how current and emerging therapies impact tissue function.

Keywords: manual lymphatic drainage, MLD, lymphedema, MRI, cancer, therapy, lymphatic

[1]Department of Physical Medicine and Rehabilitation, Vanderbilt University Medical Center, Nashville, Tennessee.
[2]Vanderbilt Dayani Center for Health and Wellness, Nashville, Tennessee.
[3]Department of Radiology, Vanderbilt University Medical Center, Nashville, Tennessee.
[4]Benchmark Physical Therapy, Chattanooga, Tennessee.
[5]Department of Surgical Oncology, Vanderbilt University Medical Center, Nashville, Tennessee.
[6]Vanderbilt School of Nursing, Nashville, Tennessee.
Departments of [7]Psychiatry, and [8]Neurology, Vanderbilt University Medical Center, Nashville, Tennessee.
[9]Department of Physics and Astronomy, Vanderbilt University, Nashville, Tennessee.

Introduction

BREAST CANCER TREATMENT-RELATED lymphedema (BCRL) arises primarily due to a mechanical insufficiency following cancer therapies, including radiation therapy and axillary lymph node removal, and it is one of the most common comorbidities in breast cancer survivors.[1] A reduction in functioning lymphatic nodes and vessels in addition to increased tissue scarring and fibrosis limit adequate processing of the lymphatic load, accumulation of protein-rich fluid in the dependent tissues, and chronic swelling of the involved arm and upper quadrant. Early detection and management is considered most effective to minimize progression of the condition, yet fundamental gaps exist in our knowledge regarding how functional changes in tissue lead to lymphedema and whether early biomarkers of lymphedema risk exist that may be used to titrate prophylactic therapies.

Complete decongestive therapy (CDT) is the clinical standard of care for lymphedema management and is comprised of four main components: (1) compression, (2) manual lymphatic drainage (MLD), (3) skin care, and (4) lymphatic flow exercises. Primarily quantified using limb volumetric assessment, MLD has been reported to have variable impact on outcomes.[2] For this reason, MLD effectiveness remains controversial as a component of CDT, resulting in uncertainty of best clinical practice for lymphedema management.

MLD has been hypothesized to temporarily (1) stimulate lymphatic fluid movement, (2) manually enhance absorption of larger interstitial proteins, and (3) redirect the lymphatic load to an uninvolved adjacent quadrant, thereby reversing or slowing condition progression and minimizing infection risk by improving tissue health. The critical barrier to evaluating MLD efficacy, along with the value of emerging lymphedema therapies and risk prevention strategies generally, is that there is a lack of internal biomarkers of lymphatic function that may serve as study end points in clinical trials of therapy impact.

Quantitative magnetic resonance imaging (MRI) measures are routinely used for evaluating treatment responses to a range of disorders, however, MRI methods capable of quantitatively evaluating tissue changes in response to lymphatic dysfunction have not yet been incorporated into condition management. Recently, efforts have focused on translating MRI approaches used for measuring circulatory dynamics in brain, breast, and liver to the lymphatic system to characterize lymph node structure[3,4] and also to generate sensitive internal markers of functional tissue changes in response to lymphatic therapy.[5,6]

We extend this work to evaluate hypothesized changes in tissue water relaxation time (T_2), a well-known MRI biomarker of tissue composition, edema, and fibrosis,[7] in healthy controls and patients with BCRL. The overreaching hypothesis is that in early stage BCRL (e.g., stages 0 and 1) before fibrosis is evident, tissue T_2 in the affected arm reduces immediately following MLD due primarily to relocation of lymphatic fluid from the affected arm to the contralateral arm. In a more advanced stage (e.g., stage 2), T_2 increases immediately after MLD in tissue of the involved arm due to a breakdown in fibrotic tissue and this effect outweighs the smaller reduction in T_2 due to lymphatic fluid relocation. In all stages, T_2 increases in the contralateral arm due to relocation of lymphatic fluid.

Quantitative T_2 measurements are paired with conventional measures of limb volume (perometry) and MRI structural fat and water imaging, and emerging measurements of bioelectrical impedance spectroscopy (BIS), and tissue dielectric constant (TDC) with the immediate goal of understanding whether quantitative MRI provides added discriminatory capacity relative to structural MRI and these non-MRI measures for determining MLD therapy efficacy and treatment optimization.

The long-term goal is to develop methodologies for accurately recording structural and functional observables of lymphatic compromise, which can serve as trial end points for future rigorous clinical trials of lymphatic dysfunction and more precise lymphedema prevention and management interventions. These methodologies would potentially extend beyond BCRL and have relevance for other conditions resulting in lymphatic dysfunction, including lipedema and adipose disorders.[8]

Methods

Volunteer demographics and enrollment

All volunteers provided informed, written consent in accordance with the Vanderbilt University Institutional Review Board. Volunteers ($n = 45$; Table 1) were enrolled as part of the prospective Imaging Noninvasively with Functional-MRI for Onset, Response, and Management of Lymphatic Impairment (INFORM^{LI}) trial (ClinicalTrials.gov Identifier: NCT02611557).

Healthy, right-handed female volunteers with no history of BCRL or lymphatic impairment ($n = 29$; age = 41.2 ± 14.8 years; age range = 23–74 years) were first evaluated to understand the normal range of the MRI index across different age ranges. The age range of healthy controls was extended relative to the BCRL range to understand a possible age dependence of the MRI measures and provide a reference for future studies. A subset of these healthy volunteers ($n = 18$; age = 51.1 ± 10.5 years; range = 37–74 years) were age-matched to patients with BCRL (stages 0–2; $n = 16$; age = 53.5 ± 10.0 years; range = 33–77 years). An additional subset of healthy controls provided repeat measurements at a different time point for reproducibility assessment ($n = 6$; age = 40.2 ± 17.8 years; range = 23–73 years).

Non-MRI measurements

Non-MRI measurements included height, weight, blood pressure (Invivo, Gainesville, FL, USA), arm volume (mL; Perometer 400NT; Pero-System, Wuppertal, Germany), TDC (MoistureMeterD; Delfin, Kuopio, Finland) and BIS (L-Dex® U400; ImpediMed, Carlsbad, CA, USA). Bilateral arm volumes were acquired using the Perometer optoelectronic device.[9,10] The total limb volume is estimated (mL) using optoelectronic infrared sensors inside a 47×47 cm frame every 4.7 mm.

Bilateral TDC measurements were incorporated to measure percent water content and its changes in the tissue at a depth of 1.5–2.5 mm.[11] The TDC measurement was repeated three times in four locations: (1) midline medial distal radioulnar joint, (2) elbow immediately anterior to medial epicondyle, (3) 4.5 cm centrally distal to axillary fold (inner upper arm), and (4) 4.5 cm centrally proximal to axillary fold

Table 1. Volunteer Demographics and Summary Values for the Three Participants Groups: Complete Group of Healthy Control Volunteers, Age-Matched Healthy Control Volunteers, and Patients with Breast Cancer Treatment-Related Lymphedema

	Age (years)	*Gender (% female)*	*BMI*	*Handedness (% right)*	*Involved side (% right)*	*Axillary lymph nodes removed (count)*	*Time since surgery (days)*	*Right arm volume (mL)*	*Left arm volume (mL)*	*L-Dex ratio*	*TDC*	*Right deep tissue T_2 (seconds)*	*Left deep tissue T_2 (seconds)*	*Right superficial T_2 (seconds)*	*Left superficial T_2 (seconds)*
All controls ($n=29$)															
Mean	41.8	100	26.6	100	NA	0	NA	4346	4284	−2.3	34.1	0.0360	0.0360	0.1478	0.1342
SD	14.7	0	6.9	0	NA	0	NA	473	490	4.1	7.8	0.0025	0.0031	0.0282	0.0353
Age-matched controls ($n=18$)															
Mean	51.1	100	27.3	100	NA	0	NA	4371	4315	−1.7	33.5	0.0363	0.0371	0.1495	0.1351
SD	10.5	0	7.8	0	NA	0	NA	516	551	4.1	7.9	0.0023	0.0032	0.0315	0.0366

	Age (years)	*Gender (% female)*	*BMI*	*Handedness (% right)*	*Involved side (% right)*	*Axillary lymph nodes removed (count)*	*Time since surgery (years)*	*Involved arm volume (mL)*	*Contra-lateral arm volume (mL)*	*L-Dex ratio*	*TDC*	*Involved deep tissue T_2 (seconds)*	*Contralateral deep tissue T_2 (seconds)*	*Involved superficial T_2 (seconds)*	*Contralateral superficial T_2 (seconds)*
Patients ($n=16$)															
Mean	53.5	100	28	100	69	17.8	5.1	4661	4448	13.4	36.9	0.0371	0.0365	0.1393	0.1385
SD	10	0	5.2	0	0	7.4	6.1	455	510	18	6.8	0.0029	0.0020	0.0347	0.0338

These non-MRI and quantitative T_2 measurements in patients represent baseline values (i.e., before MLD intervention).
BMI, body mass index; MLD, manual lymphatic drainage; MRI, magnetic resonance imaging; NA, not applicable; SD, standard deviation; TDC, tissue dielectric constant.

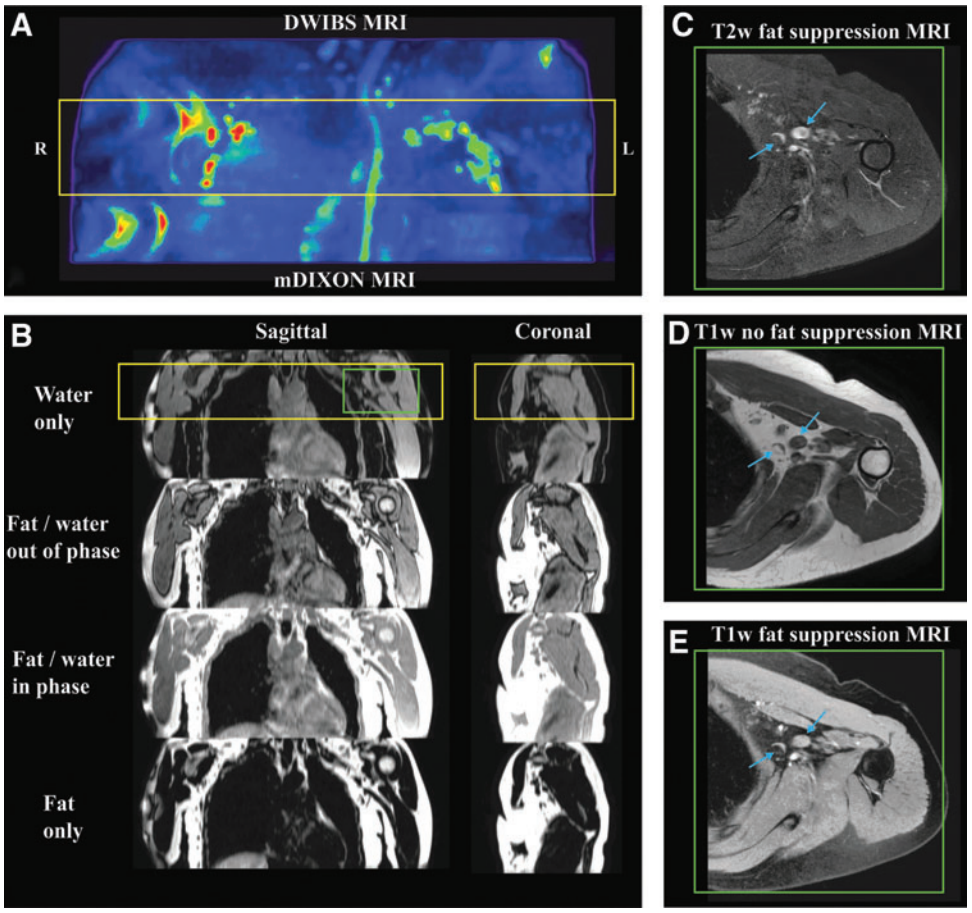

FIG. 1. Anatomical imaging and tissue regions that were the focus of the quantitative superficial and deep T_2 MRI measurements. Lymph nodes were identified on DWIBS images **(A)** (bilateral; warm colors) and surrounding tissue and fat structure were visualized on T_1-weighted mDIXON scans **(B)**. The *yellow box* denotes the approximate location of the bilateral quantitative T_2 measures. High spatial resolution T_2-weighted **(C)** and T_1-weighted **(D and E)** MRI were also used for identification of axillary regions and surrounding anatomy. *Blue arrows* denote lymph nodes. DWIBS, diffusion-weighted-inversion-with-background-suppression; mDIXON, multipoint DIXON; MRI, magnetic resonance imaging.

(lateral upper quadrant). To compare more locally with the MRI measurements, the inner upper arm measurement was used in this study, which also colocalized with edema in all patients with BCRL stages 1 and 2.

BIS was administered to measure the impedance of each arm, which scales with the extracellular fluid content of the arm.[12] The L-Dex ratio is reported as a standardized measure of the ratio of the impedance of extracellular water in the affected limb compared to the unaffected limb.[13]

Qualitative and quantitative MRI measures of tissue structure

MRI measurements were performed at 3 Tesla (Philips Medical Systems, Best, The Netherlands) using dual-channel body coil radiofrequency transmission and a 16-channel torso coil for reception. The qualitative structural MRI protocol was optimized in prior work[14] and consisted of custom diffusion-weighted-inversion-with-background-suppression imaging for large axillary node identification (spatial resolution = $3\times3\times5$ mm; b-value = 800 s/mm^2; TR/TE/TI = 7528/54/260 ms), T_1-weighted multipoint DIXON (mDIXON) for tissue and node structure (3D-gradient-echo; TR = 3.4 ms; spatial resolution = $1.0\times0.74\times2.5$ mm), high-spatial resolution fat-suppressed T_2-weighted MRI for node structure visualization (turbo-spin-echo; TR = 3500 ms; TE = 60 ms; spatial resolution = $0.4\times0.5\times5$ mm).

For quantitative T_2 measurements, a multi-echo turbo-spin-echo was applied (turbo-spin-echo; echoes = 16; range = 9–189 ms; increment = 12 ms; spatial resolution = $1.8\times1.5\times5$ mm). Additionally, B_1 field maps (3D-gradient-echo, TE/TR1/TR2 = 2.3/30/130 ms, spatial resolution = $1.8\times1.5\times5$ mm) were obtained to ensure adequate transmit radio-frequency performance, defined as obtained $B_1 \geq 75\%$ of prescribed B_1, in bilateral upper arm and axillary regions. The quantitative T_2 images were planned bilaterally over the upper arm (49 mm foot-head field-of-view) as guided by the high-spatial resolution structural imaging (Fig. 1).

MLD intervention

Following the non-MRI and MRI measurements, patients underwent a 50-minute session of MLD. The intervention was performed by a certified lymphedema physical therapist (experience = 11 years), with Lymphology Association of North America certification. MLD consisted of stimulating the bilateral supraclavicular fossae, cervical lymph nodes, shoulder collectors and axillary lymph nodes, along with

stimulating anterior and posterior axillo-axillary pathways, ipsilateral inguinal lymph nodes and axillo-inguinal pathway, deep abdominals, involved quadrant and arm applying stretch to the tissues proximal to distal toward the direction of intended lymphatic flow with temporary redirection toward uninvolved orthogonal truncal quadrants and involved posterior shoulder.[15]

MRI data analysis

The signal (S) in the multi-echo spin echo MRI data were plotted against echo time (TE) and a constrained minimization routine (fmincon; Matlab, Mathworks) was applied to simultaneously quantify the equilibrium signal intensity (S_0) and voxel-wise T_2 relaxation time according to,

$$S = S_0 \cdot e^{-TE/T_2} \quad (1).$$

Subsequently, regions of interest (ROI) encompassing (1) arm deep tissue, and (2) upper quadrant superficial tissue and subcutaneous fat were segmented from the T_2 maps (Supplementary Fig. S1; Supplementary Data are available online at www.liebertpub.com/lrb). Quantified T_2 values, separately in each region, were utilized for hypothesis testing.

Statistical considerations and hypothesis testing

The primary hypothesis is that quantitative, internal MRI measurements of tissue structure, sensitive to lymphatic fluid and fibrosis, change spatially after MLD and that these changes are more substantial than limb volume (perometry) or non-MRI measures of tissue properties including BIS and TDC. Supplementary aims were (1) to understand the discriminatory capacity of MRI measures for distinguishing edematous versus nonedematous limbs, (2) to ascertain any age-dependence of the MRI measures, and (3) to calculate reproducibility of the MRI measures in healthy controls compared with the non-MRI measures.

Descriptive statistics, including means, standard deviations (SDs), and ranges for continuous parameters were recorded. Investigations for outliers (2.5 SDs beyond mean) and assumptions for statistical analysis, for example,

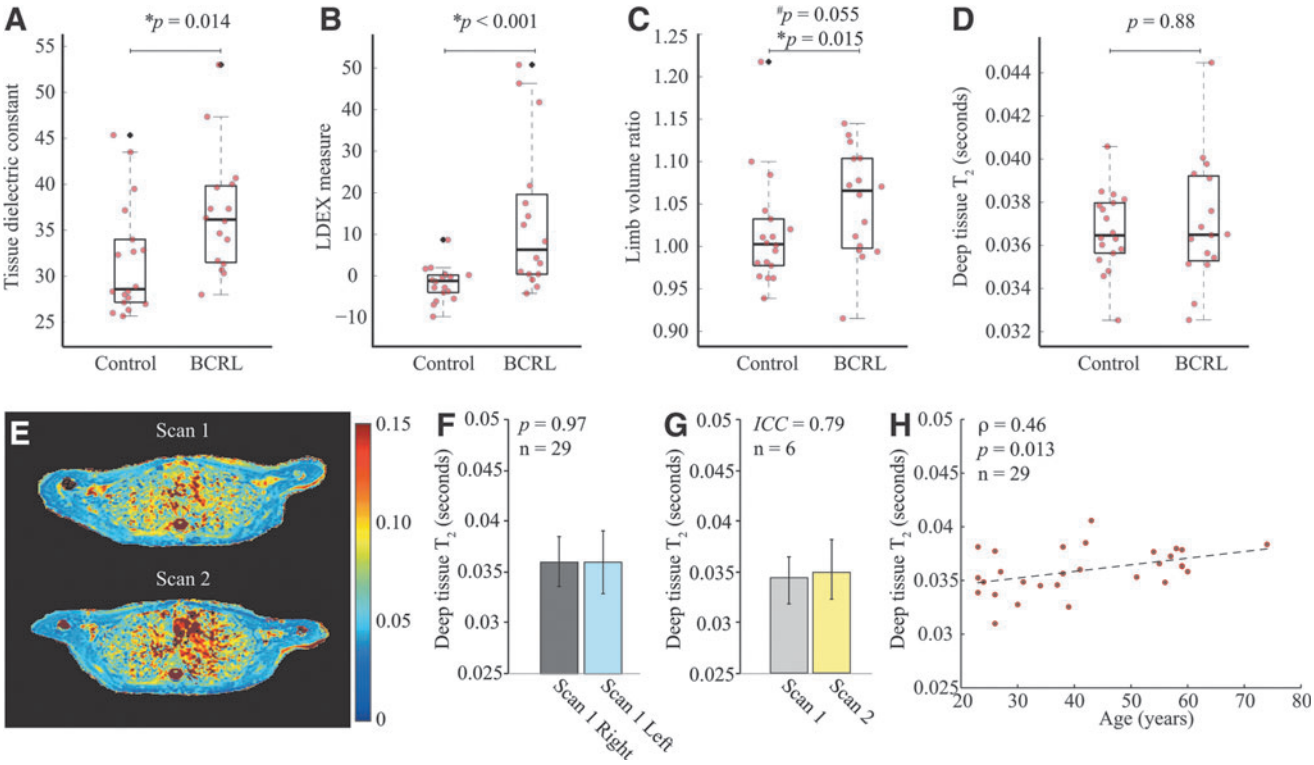

FIG. 2. Control and BCRL values of TDC **(A)**, BIS L-DEX measure **(B)**, limb volume ratio **(C)**, and deep tissue T_2 values **(D)**. TDCs are mean values including *right* and *left* arms in controls. Limb volume ratios are *right*:*left* in control volunteers and involved:contralateral in patients with BCRL. All non-MRI measures were significantly different between control and BCRL participants with the exception of limb volume ratio ($^{\#}p = 0.055$), which was only significantly different when patients with stage 0 BCRL were excluded ($^{*}p = 0.015$). Neither deep nor superficial (not shown) T_2 values were different between control and BCRL participants. p-Values denote two-sided p-values from a Wilcoxon Rank-Sum test. *Central lines* denote median, *upper and bottom solid lines* denote 75th and 25th percentile of data, and *whiskers* extend to all data not considered outliers defined as 2.5 SDs beyond the mean (*black* cross). Actual data points are overlaid as *red circles*. **(E)** One representative slice of a quantitative T_2 map (seconds) in a control participant scanned at two time points (separated by ~ 1 month) demonstrates the range of consistency in T_2 values, which are quantified **(F)** between *right* and *left* arms across all healthy control volunteers ($n = 29$) and **(G)** across the six control participants enrolled for reproducibility and ICC assessment. **(H)** A weak (Spearman's $\rho = 0.46$) but significant ($p = 0.013$) positive relationship between deep tissue T_2 and age was observed, highlighting the need to control for age in population studies that incorporate quantitative T_2 mapping of upper bodies. BCRL, breast cancer treatment-related lymphedema; BIS-L-DEX, bioimpedance spectroscopy L-DEX; ICC, intraclass correlation coefficient; TDC, tissue dielectric constant. SD, standard deviation.

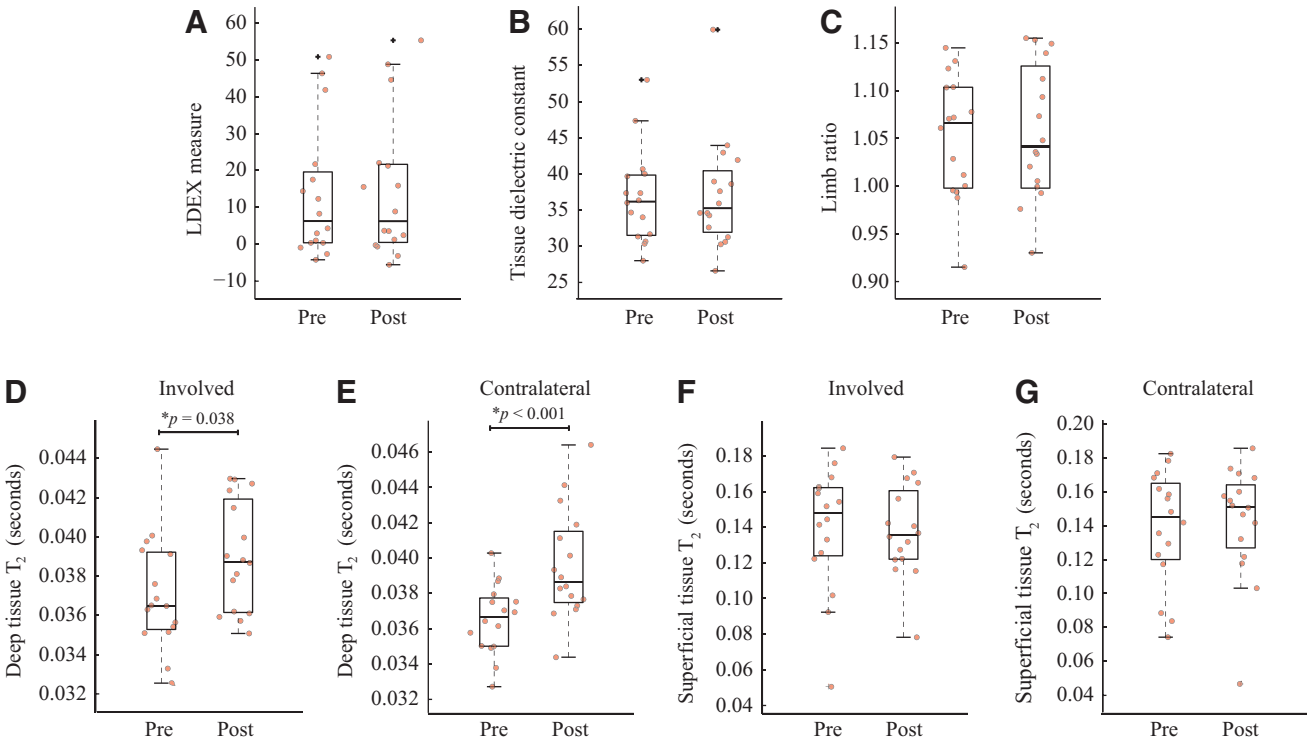

FIG. 3. Changes in study parameters pre- and post-MLD intervention in patient participants. **(A–C)** No significant change was observed in non-MRI measures pre- versus post-MLD. TDC shown is for the involved side only, however, no trend was found on the contralateral side. **(D** and **E)** In deep tissue, T_2 increases significantly on both involved and contralateral sides, whereas superficial T_2 does not change significantly on average. *p*-Values reflect two-sided results from a paired Wilcoxon Rank-Sum test. The larger range of values found in patients may provide a basis for evaluating personalized responses and is addressed in Figure 4 and the Discussion section. *Central lines* denote median, *upper and bottom solid lines* denote 75th and 25th percentile of data, and *whiskers* extend to all data not considered outliers defined as 2.5 SDs beyond the mean (*black* cross). Actual data points are overlaid as *red circles*. MLD, manual lymphatic drainage.

normality and homoscedasticity were made. To test the primary hypothesis, pre- and post-MLD measurements from each device were compared separately using a paired Wilcoxon Signed-Rank test with criteria for significance being two-sided $p < 0.05$. To test the secondary objectives, limb measurements before MLD were compared separately in involved arms of patients with BCRL to mean (e.g., right and left) arms of age-matched control participants using an unpaired Wilcoxon Rank-Sum test with criteria for significance being two-sided $p < 0.05$.

To account for absolute arm volume varying with participant body size,[16] we compared the ratio of arm volumes in

FIG. 4. A single slice taken from three patients before and after MLD intervention. All images are in radiological orientation, with the involved side on radiological *right*. For control reproducibility (Figs. 2 and 5). **(A)** A 58-year-old female with *right*-sided BCRL scanned ~5 years after 19 lymph nodes were removed when undergoing a mastectomy with lymph node dissection. Clear, focal increases in deep (*white arrows*) and superficial (*yellow arrows*) T_2 are observed after MLD. **(B)** A 57-year-old female with *right*-sided stage 1 BCRL scanned ~3 years after 24 lymph nodes were removed during a mastectomy with lymph node dissection. Similar as in **(A)**, clear regions of deep and superficial T_2 increases are observed in both quadrants. **(C)** A 59-year-old female with *right*-sided subclinical BCRL scanned ~14 years after 19 lymph nodes were removed during a mastectomy with lymph node dissection. Here, clear reductions in T_2 are observed in deep and superficial tissue T_2 on the involved side, and tissue composition changes from bilateral asymmetry pre-MLD to bilateral symmetry post-MLD. These images highlight the spatial heterogeneity of changes in MRI contrast occurring after MLD, which may not be detectable using more conventional measurements of total limb volume or emerging measurements of extracellular fluid composition. These images also are consistent with early stages of BCRL, the response to MLD is largely consistent with relocation of fluid from the involved to contralateral quadrant (T_2 lengthening). In more advanced stages of BCRL, this effect competes in a spatially dependent manner with changes in fibrosis on the involved side from pre-MLD (T_2 shortening) to post-MLD fibrosis reductions (T_2 lengthening). Heterogeneity of deep **(D and E)** and superficial **(F and G)** T_2 relaxation times in control and BCRL participants are shown. Values are SD of the quantitative T_2 over the designated region and thus reflect the heterogeneity in the measure across the region. In control participants **(D and F)**, deep and superficial T_2 are largely symmetric and vary by on average 0.01–0.02 seconds across the region. In patients with BCRL **(E and G)**, similar heterogeneity is observed in contralateral regions, however, much higher variation is observed both before and after MLD in the involved regions. These data suggest that there is a large and heterogeneous response of T_2 to MLD in the involved hemisphere. Bars denote the SD of values across all control ($n = 29$) and BCRL ($n = 16$) participants.

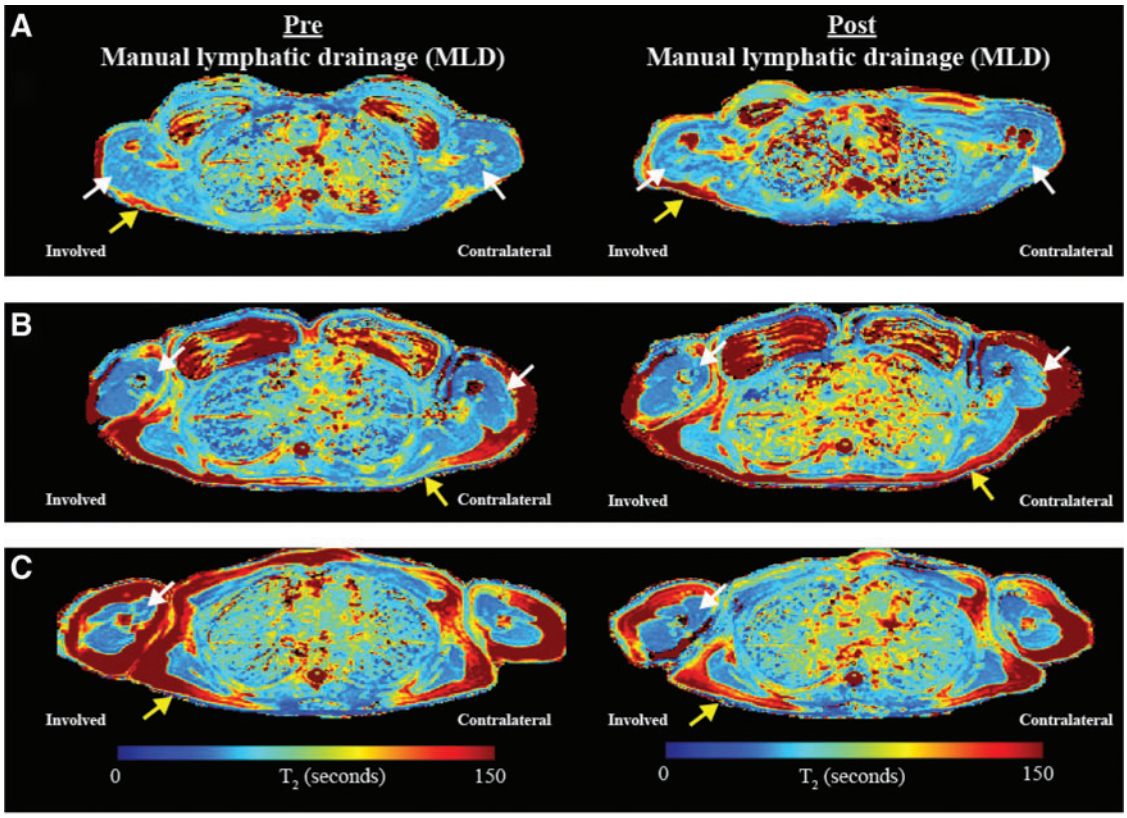

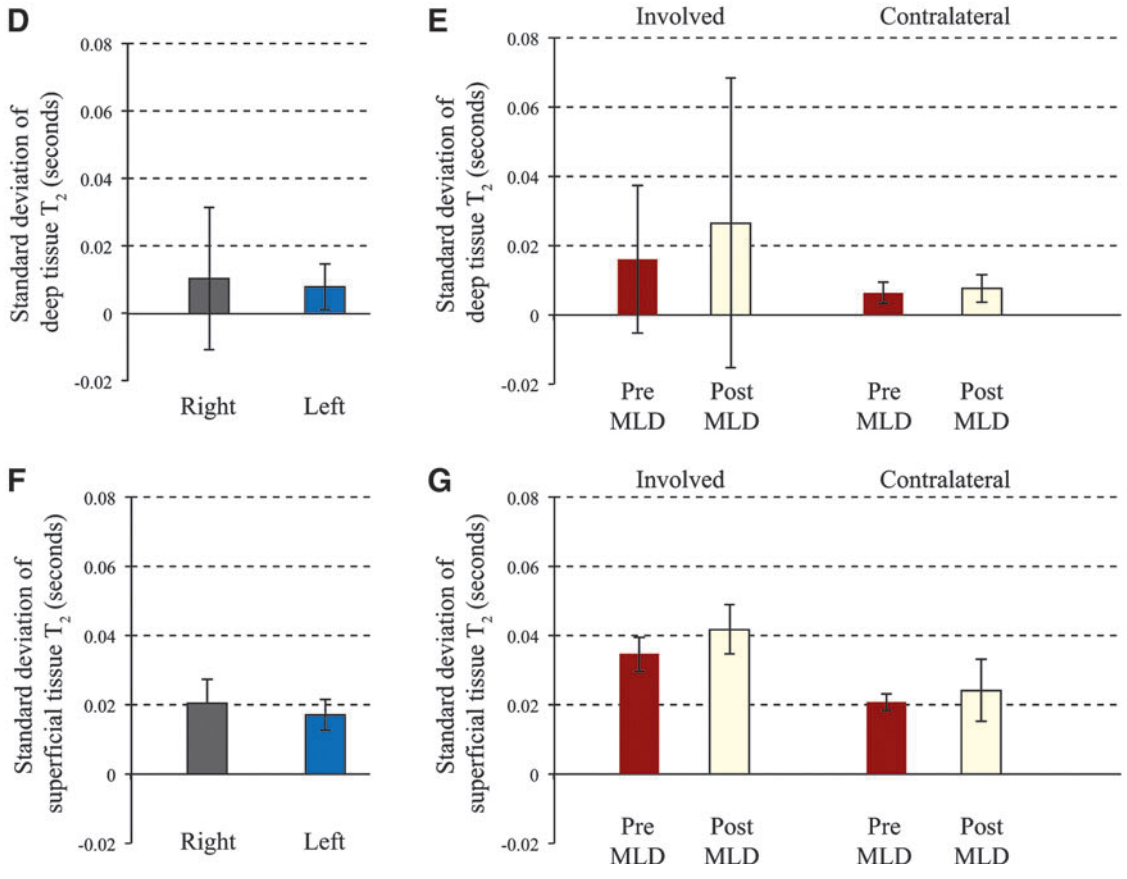

controls (i.e., right:left) to the ratio of arm volumes in patients (i.e., involved:uninvolved). To understand an effect of age on the measures, Spearman's ρ was calculated separately for each measurement as a function of age in the entire control group. Bland–Altman plots were calculated to visualize the effect of MLD on two time points, relative to differences in patients pre- and post-MLD. Finally, for reproducibility assessment in control data, intraclass correlation coefficients (ICC) were calculated for data acquired at separate time points. Two-sided p-values were reported as a conservative estimate, despite the presence of directional hypotheses.

Results

Volunteer demographics

Table 1 summarizes the volunteer demographics and study parameters for each group, which included patients with BCRL ($n=16$), age-matched controls to patients ($n=18$), and the entire control group encompassing a wider age range ($n=29$). No significant difference in age between the patients with BCRL and controls in the age-matched group was present ($p=0.50$). BCRL participants had 1–29 axillary lymph nodes removed and spanned BCRL stages 0–2 (stage 0 [$n=4$], stage 1 [$n=2$], and stage 2 [$n=10$]).

Case and control results

Figure 1 highlights the slice planning procedure and regions that were the target of imaging. Example cases of specific ROIs used are shown in Supplementary Figure S1.

Figure 2 summarizes the results of the non-MRI and quantitative deep tissue T_2 MRI measures before MLD in the control volunteers and involved arms of patients with BCRL, separately for (A) TDC, (B), BIS, (C) limb volume ratio, and (D) deep tissue T_2. TDC and BIS measurements were both significantly elevated ($p<0.05$) in patients relative to controls. A trend for elevated ratio of limb volume ($p=0.06$) was found when considering all patients (BCRL stages 0 and 2) relative to age-matched controls.

When excluding patients with preclinical lymphedema (stage 0) and considering only patients with stages 1 and 2 ($n=12$), as expected, the limb volume elevation in patients met criteria for significance as well ($p<0.01$). In contrast to the non-MRI measures, neither the deep tissue T_2 nor the superficial T_2 values differed significantly between the involved and contralateral arms of patients or between the involved arms of patients and age-matched control volunteers, a finding that is consistent with the complexity of the tissue composition in BCRL and increased free water and edema (longer T_2) counterbalancing the presence of scarring and/or fibrosis (shorter T_2).

Figure 2E shows a representative quantitative T_2 map for a control volunteer scanned at two time points demonstrating longitudinal stability of the T_2 values. Figure 2F and Table 1 depict tissue T_2 in healthy controls (deep tissue $T_2=0.036\pm0.003$ seconds; superficial tissue $T_2=0.141\pm0.03$ seconds), and deep tissue T_2 between two time points in six healthy volunteers (Fig. 2G). The ICC was found to be 0.79, consistent with an acceptable range.[17] Figure 2H shows the effect of age on the measured T_2 in healthy controls, in which a weak though significant T_2 increase with age was observed (increase = 0.06 ms/year; Spearman's $\rho=0.46$; $p=0.013$). These results summarize the range and consistency of deep tissue T_2 values in upper arms of healthy subjects, and demonstrate only a small although statistically significant increase in these measures with increasing age.

MLD therapy responses

Figure 3 summarizes the study measures before and after MLD in patients with BCRL, separately for the involved and

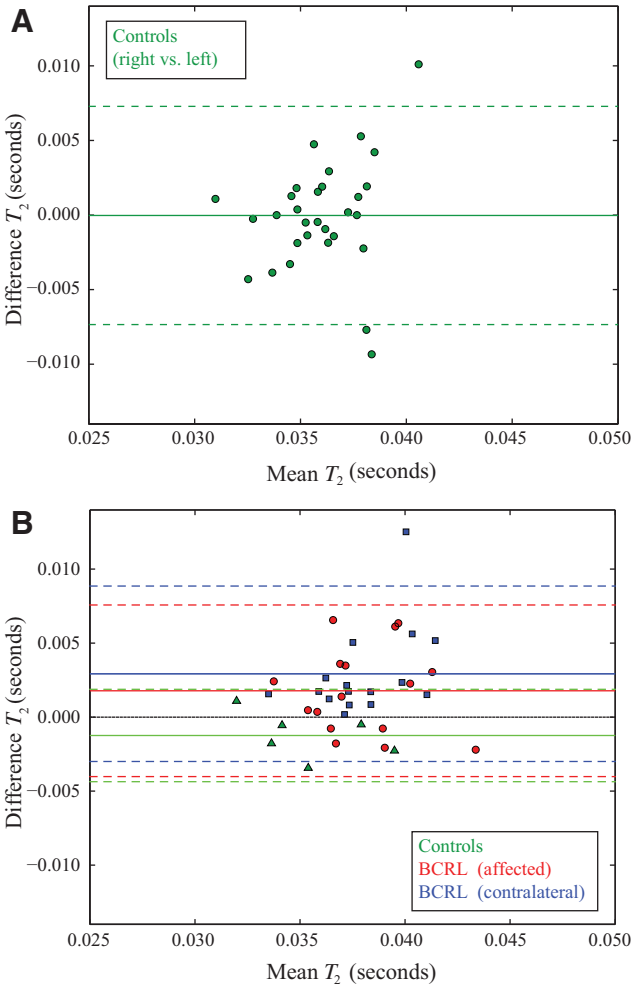

FIG. 5. **(A)** A Bland–Altman plot showing the difference (vertical axis) versus mean (horizontal axis) of T_2 values calculated in *right* and *left* arms of control volunteers, showing a mean negligible difference between *right* and *left* arm T_2. *Solid lines* signify the mean difference and *dashed lines* signify ±95% CIs. **(B)** A Bland–Altman plot showing the difference in deep tissue T_2 values before and after MLD therapy in BCRL and subset of healthy control volunteers scanned twice for reproducibility assessment. In patients with BCRL, the vertical axis depicts the difference in T_2 after MLD (post-MLD T_2 minus pre-MLD T_2) and the horizontal axis depicts the mean of pre- and post-MLD T_2 values. In controls, the vertical axis depicts the difference in T_2 values between the two scan sessions and the horizontal axis depicts the mean of the T_2 values for the two scans. The control volunteers exhibit only a small difference in quantified T_2 values between time points with relatively small CIs. In patient volunteers, the T_2 difference is larger and the 95% CIs increase, with both affected and contralateral arms exhibiting increases in T_2 after MLD therapy. 95% CI, confidence interval.

contralateral arms. A significant increase in deep tissue water T_2 was observed in the involved (pre $T_2 = 0.037 \pm 0.003$ seconds; post $T_2 = 0.039 \pm 0.003$; $p = 0.029$) and contralateral arms (pre $T_2 = 0.037 \pm 0.002$; post $T_2 = 0.040 \pm 0.002$; $p < 0.01$) after MLD.

In the superficial ROIs, an increasing trend of T_2 was noted in the contralateral side compared with a trend of reduction in the involved side. No significant difference was found in limb volume ratio, TDC, or BIS pre- versus post-MLD.

Figure 4 shows representative patient examples highlighting the spatial heterogeneity in changes in T_2 after MLD relative to the reproducibility of the T_2 measures in healthy controls scanned at two time points. Evidence of larger T_2 increases on the involved side after MLD was observed in both deep and superficial T_2 in the patients with a more advanced stage of BCRL (stage 2. Deep T_2 increase = 5.8% ± 2.9%; superficial T_2 increase = 9.8% ± 3.5%) relative to earlier stages of BCRL (stages 0 and 1 only. Deep T_2 change = 4.2% ± 3.1%; superficial T_2 change = 6.1% ± 2.3%). The SD in the T_2 measurements is quantified in Figure 4. Greater heterogeneity is observed in the involved arm of patients, which is exacerbated by the effect of MLD, compared to the contralateral arm and limbs of healthy controls.

Figure 5 presents data from all volunteers with two time points: control volunteers scanned for reproducibility assessment, and patients with BCRL scanned before and after MLD therapy. This plot confirms only a small difference in control T_2 values at the two time points, but larger T_2 value differences on both the affected and contralateral sides in the patient participants before versus after MLD.

Discussion

MLD continues to be a common component of the traditional CDT to help patients manage BCRL onset and exacerbations; however, its effectiveness and optimal utilization in the clinic remains controversial. This is largely due to difficulty detecting the specific impact MLD may have on the lymphatic system and surrounding tissue using conventional metrics.[2,18,19] Our findings revealed that non-MRI measurements (perometry, BIS, TDC) were largely confirmatory for discriminating between edematous and nonedematous limbs, yet these measures were insensitive to immediate tissue composition changes pre- versus post-MLD. However, quantitative deep tissue T_2 MRI values revealed significant changes after MLD in both the involved and contralateral quadrant.

As depicted in Figure 4, results suggest consistency with the primary study hypothesis that in more advanced stages of BCRL, breakdown of fibrotic tissue (causing T_2 lengthening) after MLD is present. These images also suggest, but do not confirm, that in early stages of BCRL, the response to MLD is largely consistent with relocation of fluid from the involved to contralateral quadrant (T_2 lengthening). Further investigation of the intervention in the different stages of BCRL is warranted given the trends noted in this study. The heterogeneous response after MLD in T_2 MRI of involved tissue indicates that a high spatial resolution internal measurement may be necessary for better understanding therapy response. These results are also consistent with previously published work suggesting MLD as a prevention intervention.[20]

Quantitative changes after MLD

Several studies have reported changes immediately after MLD. Kurz et al.[21] found changes in excretion of urinary neurohormones, specifically significant increases in histamine and serotonin, immediately following MLD in patients with lymphedema whereas no changes were found in healthy controls post-MLD.[21,22] In a pilot study, Tan et al..[23] reported near-infrared fluorescence imaging visualized lymphatic contractility improvements with an increase in both lymph velocity and propulsive frequencies immediately post-MLD for the involved and contralateral limbs in patients with known lymphedema and in both limbs of healthy controls.

Mayrovitz et al.[24] utilized TDC and tape measurements and found a decrease in percent water content measured with TDC following MLD. These TDC measurements were obtained at the subjects' most edematous sites in their legs and repeated immediately after a single MLD intervention with reported TDC percentage reductions (mean ± SD) of –9.8% ± 5.64% ($p < 0.0001$) and girth reduction of −1.5% ± 1.93% ($p < 0.01$). It is important to note that we performed TDC at predefined locations, specifically observing the upper inner arm (4.5 cm distal from axillary fold) location as the most sensitive to detecting change consistent with the quantitative T_2 ROIs. While this upper arm TDC region generally colocalized with locations of swelling in BCRL volunteers in this study, using TDC locations of greatest edema in each subject may have provided different results.

It is well documented that when volumetric measurements are obtained using a standardized method,[10,25–27] they discriminate involved from uninvolved limbs. Though volumetric measurements serve as the most commonly used clinical mechanism for quantifying treatment impact, there is question whether this indirect volumetric measurement is sensitive enough to discern the impact of the CDT components. Multiple studies have been designed in attempts to investigate volumetric changes as a response to MLD over time and some find MLD successful at reducing limb volume[28,29] while others have found no effect.[30,31]

BIS has been used to investigate its potential to identify early signs of lymphedema before overt edema is detected and before the early symptoms of arm heaviness and generalized ache.[32,33] As noted in the literature, our findings show that BIS can detect BCRL presence, yet is not sensitive as implemented to changes immediately following MLD.

Physiology of deep and superficial T_2 changes

Three Tesla MRI skeletal muscle T_2 values in rats have been reported to be 0.0327 ± 0.0013 seconds,[34] whereas human muscle has been reported to be 0.0322 ± 0.0019 seconds and 0.0357 ± 0.0023 seconds at 3 Tesla in soleus and vastus lateralis muscle, respectively.[35] Our mean values in upper arm muscle (Table 1) of 0.036 ± 0.003 seconds are largely consistent with these values and small variations may be attributable to differences in the muscle studied or species. To our knowledge, the age dependence of the deep tissue arm T_2 has not previously been reported in the literature, though it is consistent with increasing edema and tissue atrophy with age.

At 3 Tesla, T_2 relaxation is determined by spin–spin interactions, with more fluid-like environments such as free water ($T_2 = 4$–5 seconds), cerebrospinal fluid ($T_2 = 0.75$–2.0 seconds), lymphatic fluid ($T_2 = 0.5$–0.7 seconds), and blood

($T_2 = 0.013–0.175$ seconds depending on oxygenation level and hematocrit) yielding longer T_2 relative to more rigid environments such as compact bone ($T_2 < 0.0005$ seconds), muscle ($T_2 = 0.03–0.04$ seconds), and mature fibrosis ($T_2 < 0.03$ seconds).[36–44] Additionally, concentration of other molecules relevant to lymphatic function will influence the water T_2. It has been shown that in agarose phantoms water T_2 increases with increasing levels of NaCl.[45] Therefore, increasing amounts of edema and to a lesser extent sodium in muscle may lengthen T_2 whereas increasing amounts of fibrosis will reduce T_2.

Our measurements demonstrate that water T_2 increases following MLD in both the involved and contralateral arm, however, and also demonstrate that these changes are highly spatially dependent in patients and heterogeneous relative to control values in the same regions. The increase in water T_2 on the contralateral side is not surprising, and is consistent with fluid being relocated to the healthy quadrant as a result of the MLD intervention.

This is one of the first studies to our knowledge that demonstrates these expected internal changes in the tissue microenvironment with this intervention and is consistent with results from Tan et al.[23] who found an increased lymphatic fluid velocity and frequency propulsion in both the symptomatic and asymptomatic limbs using fluorescence imaging. On average, we also observed a significant increase in T_2 in the involved arm, although the statistical significance of this finding was lower. This finding may be consistent with the softening of fibrotic tissue noted in more advanced stages of BCRL and stimulation of the lymphatic and vascular circulatory systems in general as a result of the MLD intervention.

Indeed the variable effects on water T_2 are reflective of variable stages of BCRL and can be observed in specific examples of patients at each stage of disease severity (Fig. 3). BCRL stage 0 (subclinical) yielded a decrease in water T_2 on the involved side following MLD. Interestingly, in BCRL stage 0 there is no increase in T_2 in the contralateral side post-MLD, suggesting the amount of fluid needed to be reabsorbed could be largely accomplished on the involved side.

Furthermore, the results in Figure 4 illustrate tissue composition changes from bilateral asymmetry pre-MLD to more symmetry post-MLD in stage 0 displaying improved tissue health on the at-risk side. For BCRL stage 1, water T_2 decreases on the involved side and increases on the contralateral side consistent with potential rerouting of fluid to the uninvolved adjacent quadrants for reabsorption. For BCRL stage 2, water T_2 post-MLD is increased on the involved side, though only slightly, likely due to the presence of fibrosis (shorter T_2 relative to healthy tissue) that defines this staging category. The T_2 trends observed in these specific examples are representative of all patients at these stages in this cohort.

Limitations

The sample size was designed to test the hypothesis that quantitative T_2 changes are detectable in patients with BCRL relative to controls and pre- versus post-MLD, however, it is not sufficient to definitively determine how T_2 varies with specific BCRL stage in different regions. Additionally, we only performed repeat MRI immediately after MLD for quantification of immediate MLD impact; however, surveillance imaging at future time points would be useful to understand the longevity of changes and the impact repeat MLD may have on the tissue microenvironment especially for later stages of BCRL.

Finally, while a quantitative and reproducible measure, water T_2 may have multiple contributors (e.g., fibrosis and edema) and therefore provides only a surrogate marker of underlying function. In ongoing work, quantitative water T_2 measurements are paired with MRI measures of lymphatic flow[5] and interstitial protein accumulation[14] to better understand the physiological sources of these changes.

Conclusions

We have investigated the use of quantitative T_2 MRI to evaluate tissue composition in lymphadematous versus nonlymphadematous regions and to quantify microenvironment tissue changes in response to MLD intervention in patients with BCRL. Deep tissue T_2 values uniquely changed after MLD intervention and therefore may provide an attractive noninvasive internal marker to evaluate lymphatic dysfunction, associated tissue composition, and best treatment approaches.

Acknowledgments

The authors thank the National Institute of Nursing Research (NINR) within the National Institute of Health (NIH) for funding our research (1R01NR015079) resulting in this article. We are grateful to our subjects for their time, as well as Kristen George-Durrett, Leslie McIntosh, Clair Jones, Christopher Thompson, and Charles Nockowski for experimental support.

Author Disclosure Statement

No competing financial interests exist.

References

1. DiSipio T, Rye S, Newman B, Hayes S. Incidence of unilateral arm lymphoedema after breast cancer: A systematic review and meta-analysis. Lancet Oncol 2013; 14:500–515.
2. Ezzo J, Manheimer E, McNeely ML, Howell DM, Weiss R, Johansson KI, et al. Manual lymphatic drainage for lymphedema following breast cancer treatment. Cochrane Database Syst Rev 2015; 5:CD003475.
3. Korteweg MA, Zwanenburg JJ, Hoogduin JM, van den Bosch MA, van Diest PJ, van Hillegersberg R, et al. Dissected sentinel lymph nodes of breast cancer patients: Characterization with high-spatial-resolution 7-T MR imaging. Radiology 2011; 261:127–135.
4. Korteweg MA, Zwanenburg JJ, van Diest PJ, van den Bosch MA, Luijten PR, van Hillegersberg R, et al. Characterization of *ex vivo* healthy human axillary lymph nodes with high resolution 7 Tesla MRI. Eur Radiol 2011;21:310–317.
5. Rane S, Donahue PM, Towse T, Ridner S, Chappell M, Jordi J, et al. Clinical feasibility of noninvasive visualization of lymphatic flow with principles of spin labeling MR imaging: Implications for lymphedema assessment. Radiology 2013; 269:893–902.
6. Donahue MJ, Donahue PC, Rane S, Thompson CR, Strother MK, Scott AO, et al. Assessment of lymphatic impairment and interstitial protein accumulation in patients with breast cancer treatment-related lymphedema using CEST MRI. Magn Reson Med 2016;75:345–355.

7. Santyr GE. MR imaging of the breast. Imaging and tissue characterization without intravenous contrast. Magn Reson Imaging Clin N Am 1994; 2:673–690.
8. Herbst KL. Rare adipose disorders (RADs) masquerading as obesity. Acta Pharmacol Sin 2012; 33:155–172.
9. Stanton AW, Northfield JW, Holroyd B, Mortimer PS, Levick JR. Validation of an optoelectronic limb volumeter (Perometer). Lymphology 1997; 30:77–97.
10. Ancukiewicz M, Russell TA, Otoole J, Specht M, Singer M, Kelada A, et al. Standardized method for quantification of developing lymphedema in patients treated for breast cancer. Int J Radiat Oncol Biol Phys 2011; 79: 1436–1443.
11. Mayrovitz HN. Assessing free and bound water in skin at 300 MHz using tissue dielectric constant measurements with the MoistureMeterD. In: Greene AK, Brorson H, Slaven SA, eds. Lymphedema: Presentation, Diagnosis, and Treatment. New York: Springer; 2015:133–148.
12. Ridner SH, Bonner CM, Doersam JK, Rhoten BA, Schultze B, Dietrich MS. Bioelectrical impedance self-measurement protocol development and daily variation between healthy volunteers and breast cancer survivors with lymphedema. Lymphat Res Biol 2014; 12:2–9.
13. Fu MR, Cleland CM, Guth AA, Kayal M, Haber J, Cartwright F, et al. L-dex ratio in detecting breast cancer-related lymphedema: Reliability, sensitivity, and specificity. Lymphology 2013; 46:85–96.
14. Donahue MJ, Donahue PC, Rane S, Thompson CR, Strother MK, Scott AO, et al. Assessment of lymphatic impairment and interstitial protein accumulation in patients with breast cancer treatment-related lymphedema using CEST MRI. Magn Reson Med 2016; 75:345–355.
15. Zuther JE. *Lymphedema Management: The Comprehensive Guide for Practitioners*. 2nd ed. Stuttgart, Germany: Thieme; 2009.
16. Ancukiewicz M, Miller CL, Skolny MN, O'Toole J, Warren LE, Jammallo LS, et al. Comparison of relative versus absolute arm size change as criteria for quantifying breast cancer-related lymphedema: The flaws in current studies and need for universal methodology. Breast Cancer Res Treat 2012; 135:145–152.
17. Streiner DL, Norman GR. *Health Measurement Scales: A Practical Guide to Their Development and Use*. 2nd ed. Oxford and New York: Oxford University Press; 1995:viii, 231.
18. Bergmann A, da Costa Leite Ferreira MG, de Aguiar SS, de Almeida Dias R, de Souza Abrahao K, Paltrinieri EM, et al. Physiotherapy in upper limb lymphedema after breast cancer treatment: A randomized study. Lymphology 2014; 47:82–91.
19. Wilburn O, Wilburn P, Rockson SG. A pilot, prospective evaluation of a novel alternative for maintenance therapy of breast cancer-associated lymphedema [ISRCTN76522412]. BMC Cancer 2006; 6:84.
20. Torres Lacomba M, Yuste Sanchez MJ, Zapico Goni A, Prieto Merino D, Mayoral del Moral O, Cerezo Tellez E, et al. Effectiveness of early physiotherapy to prevent lymphoedema after surgery for breast cancer: Randomised, single blinded, clinical trial. BMJ 2010; 340:b5396.
21. Kurz W, Wittlinger G, Litmanovitch YI, Romanoff H, Pfeifer Y, Tal E, et al. Effect of manual lymph drainage massage on urinary excretion of neurohormones and minerals in chronic lymphedema. Angiology 1978; 29: 764–772.
22. Kurz W, Kurz R, Litmanovitch YI, Romanoff H, Pfeifer Y, Sulman FG. Effect of manual lymphdrainage massage on blood components and urinary neurohormones in chronic lymphedema. Angiology 1981; 32:119–127.
23. Tan IC, Maus EA, Rasmussen JC, Marshall MV, Adams KE, Fife CE, et al. Assessment of lymphatic contractile function after manual lymphatic drainage using near-infrared fluorescence imaging. Arch Phys Med Rehabil 2011; 92: 756.e1–764.e1.
24. Mayrovitz HN, Davey S, Shapiro E. Localized tissue water changes accompanying one manual lymphatic drainage (MLD) therapy session assessed by changes in tissue dielectric constant inpatients with lower extremity lymphedema. Lymphology 2008; 41:87–92.
25. Tidhar D, Armer JM, Deutscher D, Shyu CR, Azuri J, Madsen R. Measurement issues in anthropometric measures of limb volume change in persons at risk for and living with lymphedema: A reliability study. J Pers Med 2015; 5:341–353.
26. Armer JM. The problem of post-breast cancer lymphedema: Impact and measurement issues. Cancer Invest 2005; 23:76–83.
27. Brunelle C, Skolny M, Ferguson C, Swaroop M, O'Toole J, Taghian AG. Establishing and sustaining a prospective screening program for breast cancer-related lymphedema at the massachusetts general hospital: Lessons learned. J Pers Med 2015; 5:153–164.
28. Williams A, Vadgama A, Franks PJ, Mortimer PS. A randomized controlled crossover study of manual lymphatic drainage therapy in women with breast cancer-related lymphoedema. Eur J Cancer Care 2001; 11:254–261.
29. Cho Y, Do J, Jung S, Kwon O, Jeon JY. Effects of a physical therapy program combined with manual lymphatic drainage on shoulder function, quality of life, lymphedema incidence, and pain in breast cancer patients with axillary web syndrome following axillary dissection. Support Care Cancer 2016;24:2047–2057.
30. Andersen L, Hojris I, Erlandsen M, Andersen J. Treatment of breast-cancer-related lymphedema with or without manual lymphatic drainage—A randomized study. Acta Oncol 2000; 39:399–405.
31. Devoogdt N, Christiaens MR, Geraerts I, Truijen S, Smeets A, Leunen K, et al. Effect of manual lymph drainage in addition to guidelines and exercise therapy on arm lymphoedema related to breast cancer: Randomised controlled trial. BMJ 2011; 343:d5326.
32. Rockson SG. Detecting lymphedema: Bioimpedance spectroscopy and the tissue dielectric constant. Lymphat Res Biol 2015; 13:169.
33. Kim L, Jeon JY, Sung IY, Jeong SY, Do JH, Kim HJ. Prediction of treatment outcome with bioimpedance measurements in breast cancer related lymphedema patients. Ann Rehabil Med 2011; 35:687–693.
34. Ha DH, Choi S, Kang EJ, Park HT. Diffusion tensor imaging and T2 mapping in early denervated skeletal muscle in rats. J Magn Reson Imaging 2015; 42:617–623.
35. Forbes SC, Willcocks RJ, Triplett WT, Rooney WD, Lott DJ, Wang DJ, et al. Magnetic resonance imaging and spectroscopy assessment of lower extremity skeletal muscles in boys with Duchenne muscular dystrophy: A multicenter cross sectional study. PLoS One 2014; 9:e106435.

36. Lu H, Clingman C, Golay X, van Zijl PC. Determining the longitudinal relaxation time (T1) of blood at 3.0 Tesla. Magn Reson Med 2004; 52:679–682.
37. Rane S, Donahue P, Jordi J, Gore JC, Donahue MJ. Noninvasive characterization of lymphatic flow velocity using principles of spin labeling. International Society for Magnetic Resonance in Medicine 20th Annual Meeting and Exhibition. Abstract 575. 2012. Melbourne, Australia.
38. Jordan CD, Saranathan M, Bangerter NK, Hargreaves BA, Gold GE. Musculoskeletal MRI at 3.0 T and 7.0 T: A comparison of relaxation times and image contrast. Eur J Radiol 2013; 82:734–739.
39. Donahue MJ, Lu H, Jones CK, Edden RA, Pekar JJ, van Zijl PC. Theoretical and experimental investigation of the VASO contrast mechanism. Magn Reson Med 2006; 56: 1261–1273.
40. Manhard MK, Horch RA, Gochberg DF, Nyman JS, Does MD. *In vivo* quantitative MR imaging of bound and pore water in cortical bone. Radiology 2015; 277:221–229.
41. Melhem ER, Jara H, Eustace S. Fluid-attenuated inversion recovery MR imaging: Identification of protein concentration thresholds for CSF hyperintensity. AJR 1997; 169: 859–862.
42. Condon B, Patterson J, Jenkins A, Wyper D, Hadley D, Grant R, et al. MR relaxation times of cerebrospinal fluid. J Comput Assist Tomogr 1987; 11:203–207.
43. Hopkins AL, Yeung HN, Bratton CB. Multiple field strength *in vivo* T1 and T2 for cerebrospinal fluid protons. Magn Reson Med 1986; 3:303–311.
44. Zhao JM, Clingman CS, Narvainen MJ, Kauppinen RA, van Zijl PC. Oxygenation and hematocrit dependence of transverse relaxation rates of blood at 3T. Magn Reson Med 2007; 58:592–597.
45. Hattori K, Ikemoto Y, Takao W, Ohno S, Harimoto T, Kanazawa S, et al. Development of MRI phantom equivalent to human tissues for 3.0-T MRI. Med Phys 2013; 40:032303.

Address correspondence to:
Paula M.C. Donahue, PT, DPT, CLT-LANA
Vanderbilt Department of Physical Medicine and Rehabilitation
Vanderbilt Stallworth Rehabilitation Hospital
1500 21st Children's Way, Suite 1316
Nashville, TN 37232

E-mail: paula.m.donahue@vanderbilt.edu